Journal of Microbiology (2021) Vol. 59, No. 12, pp. 1075–1082
DOI 10.1007/s12275-021-1438-4
eISSN 1976-3794
pISSN 1225-8873

Non-mitochondrial aconitase regulates the expression of iron-uptake genes by controlling the RNA turnover process in fission yeast[§]

Soo-Yeon Cho[1,2], Soo-Jin Jung[2,3], Kyoung-Dong Kim[1*], and Jung-Hye Roe[2*]

[1]*Department of Systems Biotechnology, Chung-Ang University, Anseong 17546, Republic of Korea*
[2]*School of Biological Sciences, Seoul National University, Seoul 08826, Republic of Korea*
[3]*Center for RNA Research, Institute for Basic Science, Seoul 02841, Republic of Korea*

(Received Aug 18, 2021 / Revised Sep 13, 2021 / Accepted Sep 16, 2021)

Aconitase, a highly conserved protein across all domains of life, functions in converting citrate to isocitrate in the tricarboxylic acid cycle. Cytosolic aconitase is also known to act as an iron regulatory protein in mammals, binding to the RNA hairpin structures known as iron-responsive elements within the untranslated regions of specific RNAs. Aconitase-2 (Aco2) in fission yeast is a fusion protein consisting of an aconitase and a mitochondrial ribosomal protein, bL21, residing not only in mitochondria but also in cytosol and the nucleus. To investigate the role of Aco2 in the nucleus and cytoplasm of fission yeast, we analyzed the transcriptome of *aco2ΔN* mutant that is deleted of nuclear localization signal (NLS). RNA sequencing revealed that the *aco2ΔN* mutation caused increase in mRNAs encoding iron uptake transporters, such as Str1, Str3, and Shu1. The half-lives of mRNAs for these genes were found to be significantly longer in the *aco2ΔN* mutant than the wild-type strain, suggesting the role of Aco2 in mRNA turnover. The three conserved cysteines required for the catalytic activity of aconitase were not necessary for this role. The UV cross-linking RNA immunoprecipitation analysis revealed that Aco2 directly bound to the mRNAs of iron uptake transporters. Aco2-mediated degradation of iron-uptake mRNAs appears to utilize exoribonuclease pathway that involves Rrp6 as evidenced by genetic interactions. These results reveal a novel role of non-mitochondrial aconitase protein in the mRNA turnover in fission yeast to fine-tune iron homeostasis, independent of regulation by transcriptional repressor Fep1.

Keywords: aconitase, iron homeostasis, iron-regulatory protein, RNA degradation, fission yeast

*For correspondence. (K.D. Kim) E-mail: kdkim0122@cau.ac.kr; Tel.: +82-31-670-3359 / (J.H. Roe) E-mail: jhroe@snu.ac.kr; Tel.: +82-2-880-6706
[§]Supplemental material for this article may be found at http://www.springerlink.com/content/120956.

Introduction

During the course of evolution, organisms have devised efficient strategies for regulating the expression of their genes while sensing environmental stress (Boukouris *et al.*, 2016; Li *et al.*, 2018). Representative examples of the proteins that are involved in such regulatory mechanisms include metabolic enzymes, such as the mammalian cytosolic aconitase (Jeffery, 2015). Two aconitases are existed in higher eukaryotes such as *Caenorhabditis elegans*, *Drosophila melanogaster*, and mammals (Beinert *et al.*, 1996; Gray *et al.*, 1996; Gourley *et al.*, 2003; Lind *et al.*, 2006). Mitochondrial aconitase were widely known as mitochondrial tricarboxylic acid (TCA) cycle enzyme (Beinert *et al.*, 1996). The other aconitase senses iron deficiency and acts as an iron regulatory protein (IRP) in cytosol, controlling the expression of mRNAs of genes associated with iron homeostasis (Volz, 2008; Castello *et al.*, 2015). In iron-deficient cells, cytosolic aconitase (c-aconitase) loses its iron-sulfur (Fe-S) cluster and becomes an IRP via conformational changes (Dupuy *et al.*, 2006). IRP has the ability to bind to specific sequences of mRNAs known as iron-responsive elements (IREs). IREs are the RNA stem-loop structures located in the untranslated regions (UTRs) of mRNAs that encode proteins involved in iron homeostasis (Piccinelli and Samuelsson, 2007).

In addition to mammalian c-aconitase, aconitase B (AcnB), found in *Escherichia coli* and *Bacillus subtilis*, functions as an IRP, which binds to the mRNAs encoding proteins responsible for iron uptake and inhibits the translation of target mRNAs (Alén and Sonenshein, 1999; Benjamin and Masse, 2014). Even though the function of aconitase as an IRP is found in several organisms in bacteria and metazoan systems, the mode of action shows quite a diversity. Its role in iron regulation has not been reported among fungal systems. In *S. cerevisiae*, Aco1 is known to bind to mitochondrial DNAs and protect them from accumulating mutations and single-stranded DNA breakage (Chen *et al.*, 2005).

In fission yeast, cellular iron homeostasis is known to be regulated by transcriptional repressor Fep1. Under iron-sufficient conditions, Fep1 represses the expression of genes involved in reductive iron import (iron transport multicopper oxidase Fio1 and ferric reductase transmembrane component Frp1), siderophore transport (siderophore iron transporters Str1, Str2, and Str3) (Pelletier *et al.*, 2002, 2003), and vacuolar iron transporter Abc3 (Pouliot *et al.*, 2010). The repressive function of Fep1 is known to be assisted by Tup11 or Tup12 transcriptional co-repressor (Znaidi *et al.*, 2004; Fagerström-Billai and Wright, 2005; Pelletier *et al.*, 2005; Kim *et al.*, 2011, 2016). Fep1 incorporates Fe-S clusters which are presumably transferred from Grx4-Fra2, and the holo-form

of Fep1 can repress the expression of iron-uptake genes (Kim *et al.*, 2016). Fe-S clusters play a central role as sensors in the transcriptional regulation of iron homeostasis in fungal systems (Gupta and Outten, 2020).

Two genes encode aconitase in fission yeast *Schizosaccharomyces pombe*: *aco1* and *aco2*. Aconitase-1 (Aco1) and aconitase-2 (Aco2) proteins show ~80% sequence similarity and both have conserved cysteine residues to coordinate Fe-S cluster, which is essential for their catalytic activities. Aco1 is localized to the mitochondria with a mitochondrial targeting sequence (MTS). Unlike Aco1, Aco2 is localized not only to the mitochondria but also to the nucleus and cytosol (Jung *et al.*, 2015). Aco2 is a fusion protein consisting of N-terminal aconitase domain with MTS and C-terminal mitochondrial ribosomal domain (bL21) with a nuclear localization signal (NLS). In our previous study, we reported the role of Aco2 in mitochondrial translation (Jung *et al.*, 2015) and in forming heterochromatin in the nucleus through its association with the heterochromatin protein Chp1 (Jung *et al.*, 2019).

To investigate the roles of Aco2 in the nucleus and cytosol, we analyzed transcriptome of NLS-deleted *aco2* mutant (*aco2ΔN*) that lack nuclear and possibly cytosolic Aco2 (Jung *et al.*, 2019) and observed that the mutation caused an increase in the expression of mRNAs encoding iron transporters, whose expression is regulated by Fep1. Here, we aimed to determine the reason for the upregulation of iron transporter-coding genes in *aco2ΔN* as well as the mechanism through which Aco2 regulates the expression of iron transporter-coding genes.

Materials and Methods

Yeast strains, media, and growth conditions

The fission yeast strains used in this study are listed in Supplementary data Table S1. The yeast cells were cultured in YE-rich media and EMM-minimal media, as previously described (Forsburg and Rhind, 2006). For auxotrophic strains, supplements (adenine, leucine, and uracil, 250 mg/L each) were added to the media as appropriate. For RNA extraction, the cells were grown at 30–32°C until an OD_{600} of 0.5–1 was achieved, following which the cells were harvested.

Quantitative reverse-transcription-polymerase chain reaction (qRT-PCR)

Total RNA was extracted from cells as previously described (Kim *et al.*, 2020). To prevent contamination of genomic DNA, the DNA was removed using TURBO^{TM} DNase from the DNA-free Kit (AM1906; Thermo Fisher Scientific) according to the manufacturer's instructions. Random hexamers (100 pmol/μl) and RevertAid reverse transcriptase (Thermo Fisher Scientific) were used for cDNA synthesis as per the manufacturer's instructions. The qRT-PCR primers used in this study are shown in Supplementary data Table S2.

mRNA decay assay

Exponentially growing fission yeast cells (OD_{600} = 0.5–1) in minimal media were treated with 1,10-phenanthroline (300

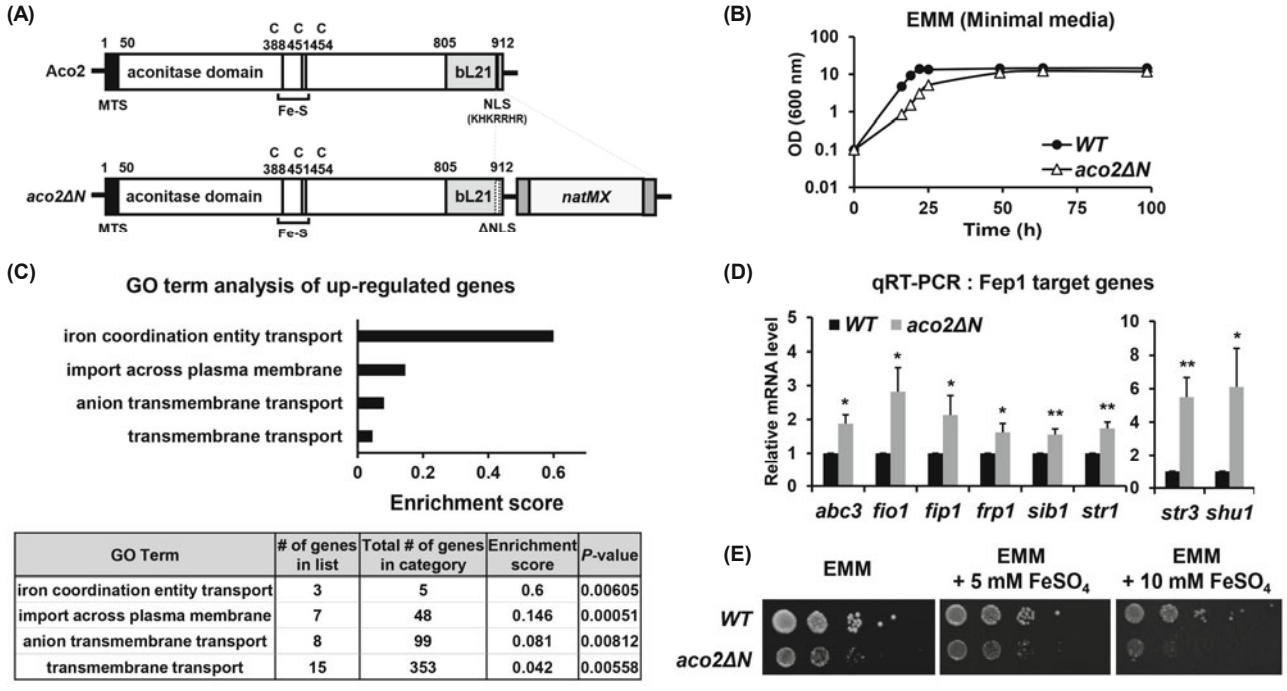

GO Term	# of genes in list	Total # of genes in category	Enrichment score	*P*-value
iron coordination entity transport	3	5	0.6	0.00605
import across plasma membrane	7	48	0.146	0.00051
anion transmembrane transport	8	99	0.081	0.00812
transmembrane transport	15	353	0.042	0.00558

Fig. 1. Effect of nuclear/cytosolic Aco2 on mRNAs for iron-uptake genes. (A) A schematic diagram of genes for the wild-type aconitase-2 (Aco2) and *aco2ΔN* mutant in *S. pombe* strains. (B) Growth curve analysis of wild-type (WT, ED972) and *aco2ΔN* mutant strains in EMM media. (C) Results of Gene Ontology (GO) term analysis using the GO TermFinder. Significantly upregulated genes in the *aco2ΔN* mutant were presented for GO categories with $p < 0.01$. The enrichment score was calculated by dividing the number of genes in the input list by the total number of genes in the GO category in *S. pombe*. (D) qRT-PCR results of iron transporter-coding mRNAs in WT (ED665) and *aco2ΔN* cells. The relative mRNA levels of the indicated genes were normalized to those of *act1* in four independent experiments. (E) Spotting assay (10-fold dilution) of WT (ED972) and *aco2ΔN* stains, with or without 5 mM or 10 mM $FeSO_4$, on EMM plates.

μg/ml) to block the transcription process. The cells were harvested at the indicated time points and immediately mixed with an equal volume of -80°C ice-cold methanol to fix the cells. Total RNA was extracted from the cells, and cDNA was synthesized using oligo dT primers (100 pmol/μl). RNA was quantified using qRT-PCR, as described above. The amount of RNA at each time point relative to that at $t = 0$ was plotted.

Chromatin Immunoprecipitation (ChIP)

ChIP was performed as previously described (Kim *et al.*, 2020), with minor modifications. FLAG-tagged proteins were purified using an anti-DDDDK-tag antibody (MBL) and A/G agarose (Santa Cruz Biotechnology). The enrichment of tagged proteins on the target genes was examined with qRT-PCR using the primers described in Supplementary data Table S2.

UV crosslinking RNA immunoprecipitation (CLIP) analysis

CLIP analysis was performed as described in a previous study (Satoh *et al.*, 2009), with some modifications. The cells expressing the FLAG-tagged protein were harvested at OD_{600} = 0.5–0.8 and UV crosslinked using Stratalinker (254 nm, 20,000 J/cm^2 for 30 sec, 2 times). The crosslinked cells were then disrupted with beads beater in a lysis buffer (25 mM HEPES-KOH; pH 7.5, 150 mM KCl, 2 mM $MgCl_2$, 10 mM PMSF, 200 U/ml RNase inhibitor, 0.1% NP-40, 1 mM DTT, and a proteinase inhibitor cocktail). The contaminated DNA was removed by incubation with TURBO™ DNase (Thermo Fisher Scientific) for 30 min at 30°C. For IP, the cell extracts were incubated with A/G agarose (Santa Cruz Biotechnology) and 2 μl of anti-DDDDK-tag antibody (MBL) for 3–4 h at 4°C. Immunoprecipitated beads were then washed four times with the wash buffer (25 mM HEPES-KOH; pH 7.5, 150 mM KCl, and 2 mM $MgCl_2$) and RNA was eluted by incubation with 150 μl of elution buffer at 65°C for 5 min, 2 times. The supernatants were incubated with proteinase K at 42°C for 30 min, and RNA was further prepared by phenol extraction and ethanol precipitation. For qRT-PCR analysis, cDNA was synthesized using gene-specific RT (GST) primers (Supplementary data Table S2).

Statistical analysis

Data in this study were presented as the mean ± SEM of more than three independent experiments. Statistical significance (p-value) was determined by Student's t-test (***$p < 0.001$, **$p < 0.01$, *$p < 0.05$, ns $p > 0.05$).

Results

Growth defects and upregulation of Fep1-regulon genes in *aco2ΔN* mutant

To investigate the role of Aco2 in the nucleus and possibly

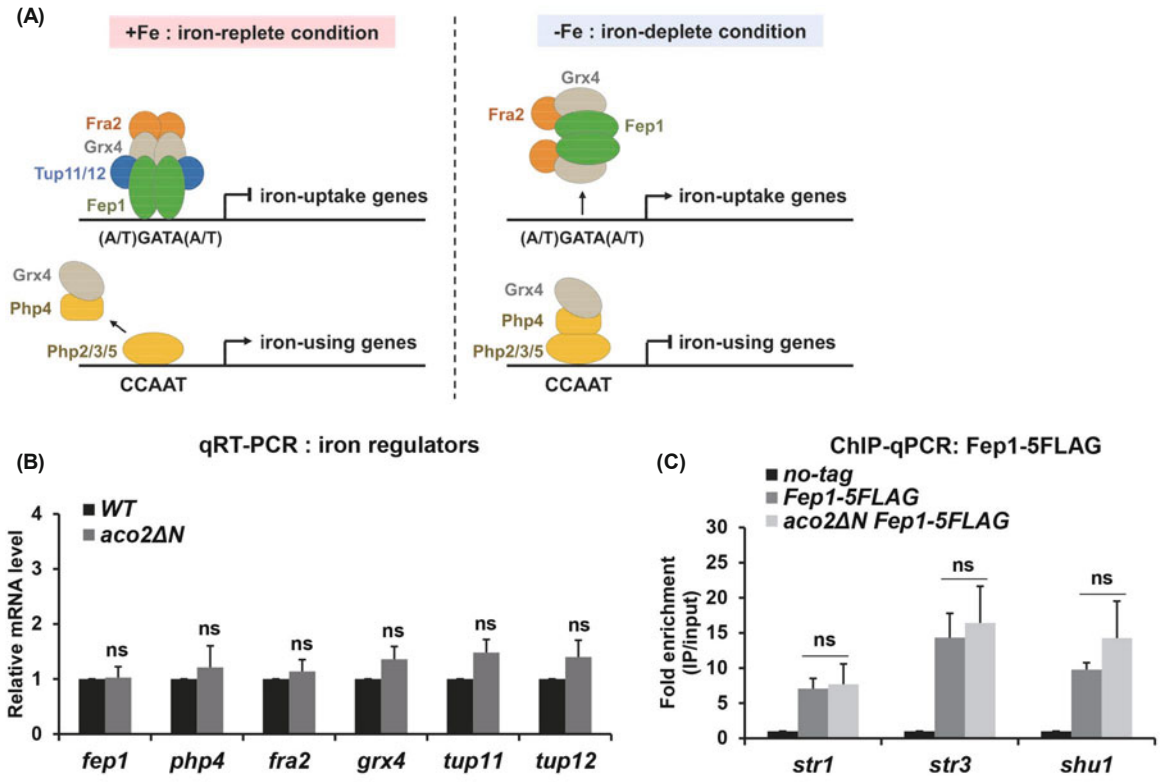

Fig. 2. Transcriptional regulation of iron transporter-coding genes in *aco2ΔN*. (A) A schematic model of iron homeostasis in *S. pombe*. Iron-uptake and regulation by Fep1 and other co-regulators are shown. (B) Transcript levels of genes encoding Fep1 and other co-regulators in WT (ED665) and *aco2ΔN* cells. Expression levels of iron transporter-coding genes relative to *act1* were determined by qRT-PCR. Average values from three independent experiments were presented. (C) Chromatin immunoprecipitation (ChIP)-qPCR analysis of Fep1-5FLAG at the promoter regions of iron transporter-coding genes (*str1*, *str3*, and *shu1*) in WT and *aco2ΔN* strains. Fold enrichments over the no-tag control (WT, ED972) from three independent experiments are shown.

in the cytosol, we analyzed NLS-deleted *aco2ΔN* mutant (Fig. 1A). We first examined the growth rates of cells in minimal medium (EMM) and revealed that the doubling rate and final optical density (OD_{600}) of the *aco2ΔN* mutant were slightly lower than those of the wild-type strain in EMM (Fig. 1B). To further examine the role of nuclear/cytosolic Aco2 on gene expression, we subjected the cells cultured in EMM to RNA-sequencing (RNA-seq) analysis (Fig. 1C). Compared with the wild-type transcriptome, 164 protein-coding genes were differentially expressed in the *aco2ΔN* mutant; 98 genes were downregulated and 66 genes were upregulated. We categorized these genes using an online tool; Gene Ontology (GO) TermFinder (https://go.princeton.edu/cgi-bin/GOTermFinder). The result demonstrated that the upregulated genes were significantly ($p < 0.01$) enriched in several biological processes, such as transmembrane transport and iron transport (Fig. 1C). In particular, the iron transporter category was the most significantly enriched in the *aco2ΔN* mutant compared with the wild-type (Fig. 1C). Based on this result, we focused on the regulation of iron transporter-coding genes by Aco2.

Confirmation of RNA-seq results by qRT-PCR revealed that the expression levels of all genes regulated by Fep1 were significantly increased in the *aco2ΔN* mutant (Fig. 1D). We summarized the list of Fep1-regulon genes and differences in their expression levels detected by RNA-seq and qRT-PCR (Supplementary data Table S3). To investigate whether the increased expression of Fep1-target genes in the *aco2ΔN* mutant affects the viability of cells under excess iron conditions, we conducted a spotting assay and observed that the *aco2ΔN* mutation indeed decreased viability on EMM containing up to 10 mM $FeSO_4$ (Fig. 1E), indicating that the role of nuclear/cytosolic Aco2 on the expression of Fep1-regulated iron transporter genes is physiologically important to maintain iron homeostasis required for cell viability.

Fep1-independent regulation of iron-uptake gene expression by Aco2

Next, we examined the expression levels of Fep1 and its known co-repressors, including Tup11, Tup12, Php4, Fra2, and Grx4, that function in the transcriptional regulation of Fep1-target genes (Fig. 2A) (Pelletier *et al.*, 2005; Mercier *et al.*, 2008; Kim *et al.*, 2011, 2016; Jacques *et al.*, 2014; Mourer *et al.*, 2015). The result indicated no significant differences between the wild-type and *aco2ΔN* mutant in the expression level of genes for these components in the transcriptional regulatory pathway (Fig. 2B). We further examined the binding enrichment of Fep1 at the promoter regions of known Fep1-target genes encoding siderophore iron transporters (str1 and str3), and cell-surface heme acquisition protein (shu1), that are the most upregulated in *aco2ΔN* strain from RNA-seq result, via chromatin immunoprecipitation (ChIP)-qPCR analysis. The result revealed no significant difference in the binding enrichment of Fep1 at the target loci between the wild-type and the mutant (Fig. 2C). These data suggest that Aco2 may affect not the transcription but the post-transcriptional stability of iron-ptake mRNAs, independent of Fep1-regulatory pathway.

Role of Aco2 in the degradation of iron-uptake mRNAs

To investigate whether the stability of iron-uptake mRNAs changed in the *aco2ΔN* mutant, mRNA decay assay using 1,10-phenanthroline was carried out as described in the 'Ma-

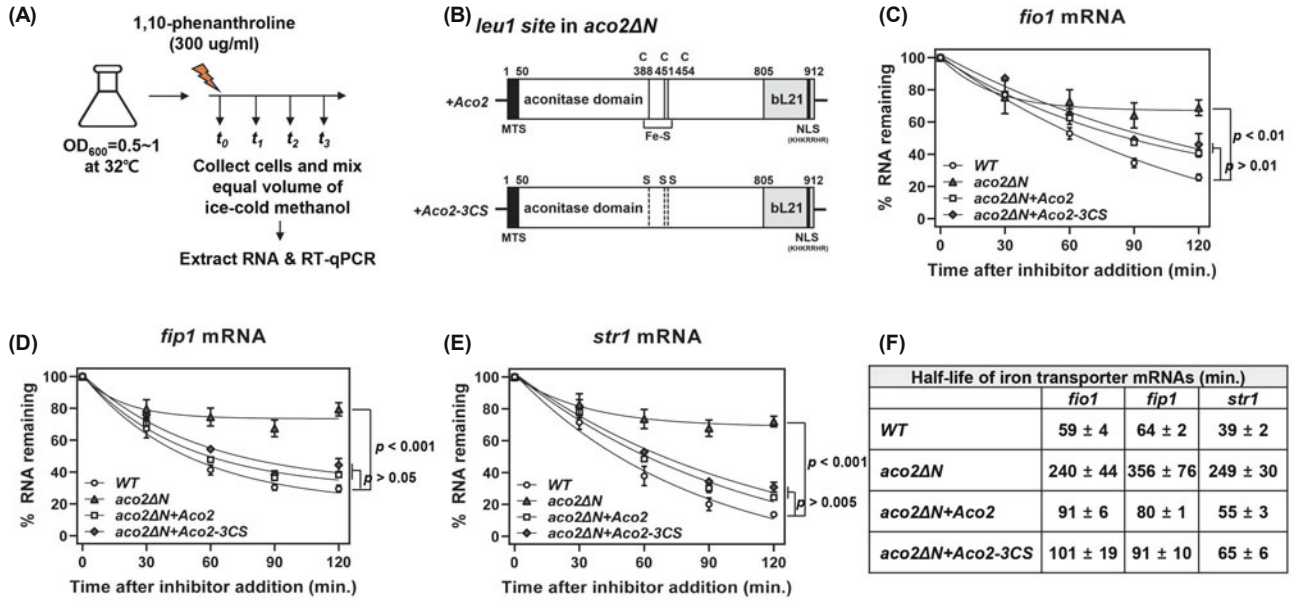

Fig. 3. Role of Aco2 in facilitating degradation of mRNAs encoding iron transporters. (A) Experimental scheme of the mRNA decay assay. Cells were treated with 1,10-phenanthroline (300 μg/ml) as transcriptional inhibitor and collected at different time span for RNA analysis. (B) A schematic diagram of complementation of *aco2ΔN* strain by the wild-type (+*Aco2*) and mutant *aco2* gene whose three conserved cysteines were substituted with serines (+*Aco2-3CS*). The complementing genes were inserted in the *leu1* site of *aco2ΔN* mutant. (C–E) mRNA decay profile of the wild-type, *aco2ΔN* and complemented strains. Graph symbols of WT (white circle), *aco2ΔN* (gray triangle), *aco2ΔN+Aco2* (white square) and *aco2ΔN+Aco2-3CS* (gray diamond) represent average values of three independent experiments with SEM. The *p*-value was calculated by comparing with the wild-type value at $t = 120$, respectively. (F) Measured values of the mRNA half-lives for *fio1*, *fip1,* and *str1* were presented for the wild-type and mutant strains with or without complementation.

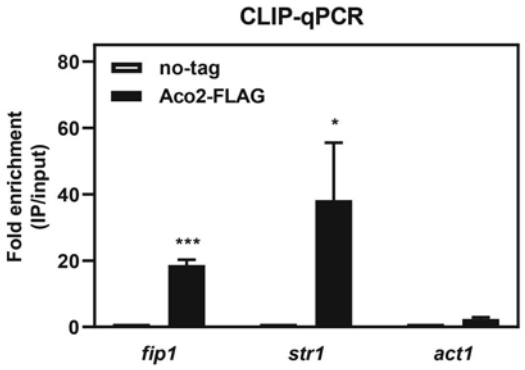

Fold enrichment over no-tag		
fip1	*str1*	*act1*
18.65 ± 1.64	38.25 ± 17.26	2.44 ± 0.47

Fig. 4. CLIP-qPCR analysis of physical interaction between Aco2 and iron-uptake mRNAs. The enrichment of *fip1* and *str1* mRNAs after UV cross-linking RNA immunoprecipitation (CLIP) with antibody against FLAG-tagged Aco2 was measured by qRT-PCR, using *act1* as the negative control. Data were presented as mean values of fold enrichment relative to the no-tag control (WT, ED665) from five independent experiments.

terials and Methods. The level of mRNAs for *fio1*, *fip1*, and *str1* genes was quantified by qRT-PCR and the relative amount of remaining mRNA was plotted at each time point relative to $t = 0$ (Fig. 3A). We selected *fio1*, *fip1*, and *str1* among Fep1-target genes for the later experiments since the basal expression of those genes in normal condition were relatively stable based on FPKM values from our RNA-seq result. Interestingly, the degradation rates of these mRNAs were decreased in the *aco2ΔN* mutant compared with the wild-type strain (Fig. 3C–E) and the mRNA half-lives increased by more than 4- to 6-fold in the mutant (Fig. 3F).

The defects in the degradation of iron-uptake mRNAs in the *aco2ΔN* mutant was complemented by the wild-type *aco2* gene which was integrated in the *leu1* locus (Fig. 3B). Since the mammalian cytosolic aconitase becomes an IRP when it loses Fe-S cluster, we investigated whether Aco2 in *S. pombe* functions in mRNA decay independently of Fe-S cluster. Substitution mutation of three conserved cysteine residues at 388, 451, and 454 positions that can coordinate Fe-S cluster in aconitase to serines (Aco2-3CS) was created (Fig. 3B) and introduced into the *aco2ΔN* mutant strain. The complementation showed similar effect as the wild-type gene (Fig. 3C–F). This data implies that the role of Aco2 in regulating mRNA stability does not require Fe-S cluster.

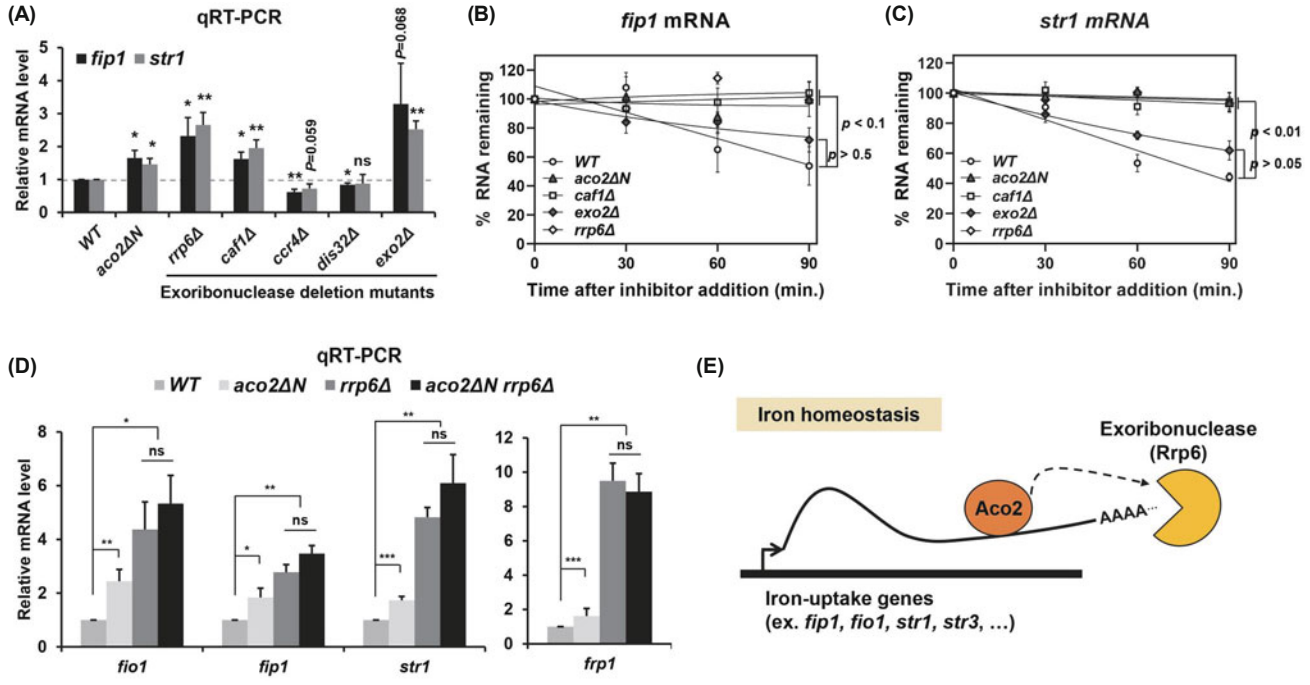

Fig. 5. Relationship between Aco2 and exoribonucleases in the degradation of iron-uptake mRNAs. (A) Relative expression levels of iron transporter-coding mRNAs in WT (ED665), *aco2ΔN*, and five exoribonuclease mutant strains determined by qRT-PCR. Expression levels of *fip1* and *str1* mRNAs relative to the *act1* mRNA in the indicated strains were presented from three independent experiments. (B and C) The mRNA decay analysis of *fip1* and *str1* mRNAs in the WT (white circle), *aco2ΔN* (gray triangle), *caf1Δ* (white square), *exo2Δ* (gray diamond), and *rrp6Δ* (white diamond) strains. Data represent the average values of three independent experiments with SEM. The *p*-value was calculated by comparing with the wild-type value at $t = 90$, respectively. (D) qRT-PCR analysis of iron transporter-coding mRNAs in WT (ED665), *aco2ΔN*, *rrp6Δ*, and *aco2ΔN rrp6Δ* cells to investigate genetic interaction between Aco2 and Rrp6. Mean values from more than three independent experiments were presented. (E) A schematic model of Aco2-mediated mRNA decay of iron uptake genes. Aco2 acts as the RNA-binding protein and mediates the degradation of iron transporter-coding mRNAs by exoribonuclease such as Rrp6.

Binding of Aco2 to iron-uptake mRNAs

We performed ultraviolet (UV) crosslinking RNA immunoprecipitation (CLIP) analysis to examine physical binding of Aco2 to iron-uptake mRNAs. Cells expressing FLAG-tagged Aco2 (Aco2-5FLAG, [Jung *et al.*, 2019]) were grown to OD_{600} of 0.5–1 in EMM media, followed by UV crosslinking. Wild-type cells were used in parallel as no-tag control. After immunoprecipitation (IP) with anti-DDDDK-tag antibody, cDNAs were synthesized using gene-specific reverse transcription (RT) primers for *fip1* and *str1* mRNAs. The mRNA binding activity of Aco2 estimated by qRT-PCR revealed that the enrichment of *fip1* and *str1* mRNAs was significantly higher in cells expressing Aco2-FLAG than in the no-tag control cells (Fig. 4). This indicates physical interaction of Aco2 with mRNAs encoding iron transporters.

Exoribonucleases involved in the degradation of iron-uptake mRNAs

To elucidate the role of Aco2 in the degradation of iron transporter-coding mRNAs, we examined the functional relationship of Aco2 with known RNA processing enzymes in *S. pombe.* Based on the PomBase (pombase.org) annotation, we selected some ribonucleases, such as Caf1, Ccr4, Dis32, Exo2, and Rrp6, which are involved in mRNA catabolic processes. We then examined the mRNA levels of iron-uptake genes in five available exoribonuclease mutants relative to the wild-type. The result demonstrated that the mRNA levels of *fip1* and *str1* were significantly increased in *caf1Δ*, *exo2Δ*, and *rrp6Δ* mutants (Fig. 5A). Thus, we further analyzed the effect of three RNA processing enzymes (Caf1, Exo2, and Rrp6) on mRNA stability. The mRNA decay assay demonstrated that the degradation of *fip1* and *str1* mRNAs was delayed not only in *aco2ΔN* mutant strain but also in *caf1Δ* and *rrp6Δ* (Fig. 5B and C), suggesting that exoribonucleases, such as Caf1 and Rrp6, participate in the degradation of iron-uptake mRNAs.

Functional relevance of Aco2 with Rrp6

Rrp6 has been reported to target mRNAs of the iron-uptake and meiotic genes (Mukherjee *et al.*, 2016). To investigate interaction between Rrp6 and Aco2, we examined their genetic interaction by monitoring expression of iron-uptake genes in the *aco2ΔN rrp6Δ* double mutant. The qRT-PCR results indicated that there was no significantly additive increase in mRNA expression of iron transporter-coding genes in the *aco2ΔN rrp6Δ* double mutant (Fig. 5D), suggesting that Aco2 and Rrp6 may participate in the same degradation pathway.

We further tried to investigate whether Rrp6 and Aco2 share other target mRNA groups in addition to the iron-uptake function. Rrp6 is a subunit of the nuclear exosome that degrades early meiotic genes during vegetative growth (Harigaya *et al.*, 2006; Touat-Todeschini *et al.*, 2017; Telekawa *et al.*, 2018; Shichino *et al.*, 2020). RNA-seq results were visualized using a heatmap (Supplementary data Fig. S1) for comparison analyses among the data acquired from the current study as well as from previous studies (Mukherjee *et al.*, 2016; Hocquet *et al.*, 2018). We found that the meiotic genes only accumulated in the *rrp6Δ* strain but not in the *aco2ΔN* mutant strain (Supplementary data Fig. S1A). However, Fep1-regulons accumulated in both *aco2ΔN* and *rrp6Δ* mutant strains (Supplementary data Fig. S1B). These RNA-seq data suggest that Aco2 regulates the mRNA turnover of Fep1-regulated genes, but not for meiotic genes, in the same exosome pathway involving exonucleases, such as Rrp6 (Fig. 5E).

Discussion

Cells possess diverse mechanisms to regulate the expression of genes at the transcriptional and post-transcriptional levels. In fission yeast, the meiotic gene transcripts are degraded by exosome complexes during vegetative growth (Harigaya *et al.*, 2006; Yamamoto, 2010; Yamanaka *et al.*, 2010; Chen *et al.*, 2011; Yamashita *et al.*, 2012; Egan *et al.*, 2014; Kilchert *et al.*, 2016; Shichino *et al.*, 2020). The determinant of selective removal (DSR) motif on the transcripts of meiotic genes is recognized by Mmi1, an YTH-family RNA-binding protein. Meanwhile, the exosome complexes, including two 3′–5′ exonucleases, Rrp6 and Dis3, target the Mmi1-bound regions (Harigaya *et al.*, 2006; Yamashita *et al.*, 2012; Kilchert *et al.*, 2016). Thus, RNA exosomes play crucial roles in the regulation of meiotic genes. Recently, several genes other than meiotic genes have been identified as exosome targets using RNA-seq analyses in the *rrp6Δ* mutant strain (Mukherjee *et al.*, 2016). One category of genes includes those that encode iron transporters that do not contain the DSR motif and are independent of the Mmi1 pathway (Mukherjee *et al.*, 2016). However, the mechanism through which the transcripts of iron transporter-coding genes are regulated at the post-transcriptional level remained poorly understood.

Here, we demonstrated that nuclear/cytosolic Aco2 was involved in the regulation of iron homeostasis by mediating degradation of iron transporter-coding mRNAs in fission yeast. This regulation is independent of Fep1-mediated transcriptional regulation. Physical binding of Aco2 to the mRNAs encoding iron transporters, and the genetic interaction of Aco2 with Rrp6, led us to propose Aco2-mediated interaction of iron-transporter mRNAs with exosome pathway that involves Rrp6 (Fig. 5E). Although we propose a functional relationship between Aco2 and Rrp6, and possibly with other components of the exosome complex, physical interactions among them need be elucidated to better understand the mechanism of action. How Aco2 recognizes iron-uptake mRNAs and how this recognition is controlled by iron-availability await further investigation.

Acknowledgements

This work was supported by grants from the National Research Foundation of Korea (NRF) to K.K. (2019R1A4A-1024764). SY Cho was supported by the BK21-Plus fellowship at SNU and the BK21 FOUR fellowship at CAU.

Conflict of Interest

The authors declare that they have no conflict of interest.

Author Contributions

Conception and experimental design: S. C., K. K., and J. R.; methodology and data acquisition: S. C. and S. J.; paper writing: S. C., K. K., and J. R.

References

Alén, C. and Sonenshein, A.L. 1999. *Bacillus subtilis* aconitase is an RNA-binding protein. *Proc. Natl. Acad. Sci. USA* **96**, 10412–10417.

Beinert, H., Kennedy, M.C., and Stout, C.D. 1996. Aconitase as iron-sulfur protein, enzyme, and iron-regulatory protein. *Chem. Rev.* **96**, 2335–2374.

Benjamin, J.A. and Masse, E. 2014. The iron-sensing aconitase B binds its own mRNA to prevent sRNA-induced mRNA cleavage. *Nucleic Acids Res.* **42**, 10023–10036.

Boukouris, A.E., Zervopoulos, S.D., and Michelakis, E.D. 2016. Metabolic enzymes moonlighting in the nucleus: metabolic regulation of gene transcription. *Trends Biochem. Sci.* **41**, 712–730.

Castello, A., Hentze, M.W., and Preiss, T. 2015. Metabolic enzymes enjoying new partnerships as RNA-binding proteins. *Trends Endocrinol. Metab.* **26**, 746–757.

Chen, H.M., Futcher, B., and Leatherwood, J. 2011. The fission yeast RNA binding protein Mmi1 regulates meiotic genes by controlling intron specific splicing and polyadenylation coupled RNA turnover. *PLoS ONE* **6**, e26804.

Chen, X.J., Wang, X., Kaufman, B.A., and Butow, R.A. 2005. Aconitase couples metabolic regulation to mitochondrial DNA maintenance. *Science* **307**, 714–717.

Dupuy, J., Volbeda, A., Carpentier, P., Darnault, C., Moulis, J.M., and Fontecilla-Camps, J.C. 2006. Crystal structure of human iron regulatory protein 1 as cytosolic aconitase. *Structure* **14**, 129–139.

Egan, E.D., Braun, C.R., Gygi, S.P., and Moazed, D. 2014. Post-transcriptional regulation of meiotic genes by a nuclear RNA silencing complex. *RNA* **20**, 867–881.

Fagerström-Billai, F. and Wright, A.P. 2005. Functional comparison of the Tup11 and Tup12 transcriptional corepressors in fission yeast. *Mol. Cell. Biol.* **25**, 716–727.

Forsburg, S.L. and Rhind, N. 2006. Basic methods for fission yeast. *Yeast* **23**, 173–183.

Gourley, B.L., Parker, S.B., Jones, B.J., Zumbrennen, K.B., and Leibold, E.A. 2003. Cytosolic aconitase and ferritin are regulated by iron in *Caenorhabditis elegans*. *J. Biol. Chem.* **278**, 3227–3234.

Gray, N.K., Pantopoulos, K., Dandekar, T., Ackrell, B.A., and Hentze, M.W. 1996. Translational regulation of mammalian and *Drosophila* citric acid cycle enzymes via iron-responsive elements. *Proc. Natl. Acad. Sci. USA* **93**, 4925–4930.

Gupta, M. and Outten, C.E. 2020. Iron–sulfur cluster signaling: the common thread in fungal iron regulation. *Curr. Opin. Chem. Biol.* **55**, 189–201.

Harigaya, Y., Tanaka, H., Yamanaka, S., Tanaka, K., Watanabe, Y., Tsutsumi, C., Chikashige, Y., Hiraoka, Y., Yamashita, A., and Yamamoto, M. 2006. Selective elimination of messenger RNA prevents an incidence of untimely meiosis. *Nature* **442**, 45–50.

Hocquet, C., Robellet, X., Modolo, L., Sun, X.M., Burny, C., Cuylen-Haering, S., Toselli, E., Clauder-Münster, S., Steinmetz, L., Haering, C.H., *et al.* 2018. Condensin controls cellular RNA levels through the accurate segregation of chromosomes instead of directly regulating transcription. *eLife* **7**, e38517.

Jacques, J.F., Mercier, A., Brault, A., Mourer, T., and Labbé, S. 2014. Fra2 is a co-regulator of Fep1 inhibition in response to iron starvation. *PLoS ONE* **9**, e98959.

Jeffery, C.J. 2015. Why study moonlighting proteins? *Front. Genet.* **6**, 211.

Jung, S.J., Choi, Y., Lee, D., and Roe, J.H. 2019. Nuclear aconitase antagonizes heterochromatic silencing by interfering with Chp1 binding to DNA. *Biochem. Biophys. Res. Commun.* **516**, 806–811.

Jung, S.J., Seo, Y., Lee, K.C., Lee, D., and Roe, J.H. 2015. Essential function of Aco2, a fusion protein of aconitase and mitochondrial ribosomal protein bL21, in mitochondrial translation in fission yeast. *FEBS Lett.* **589**, 822–828.

Kilchert, C., Wittmann, S., and Vasiljeva, L. 2016. The regulation and functions of the nuclear RNA exosome complex. *Nat. Rev. Mol. Cell Biol.* **17**, 227–239.

Kim, E.J., Cho, Y.J., Chung, W.H., and Roe, J.H. 2020. The role of Rsv1 in the transcriptional regulation of genes involved in sugar metabolism for long-term survival. *FEBS J.* **287**, 878–896.

Kim, K.D., Kim, H.J., Lee, K.C., and Roe, J.H. 2011. Multi-domain CGFS-type glutaredoxin Grx4 regulates iron homeostasis via direct interaction with a repressor Fep1 in fission yeast. *Biochem. Biophys. Res. Commun.* **408**, 609–614.

Kim, H.J., Lee, K.L., Kim, K.D., and Roe, J.H. 2016. The iron uptake repressor Fep1 in the fission yeast binds Fe-S cluster through conserved cysteines. *Biochem. Biophys. Res. Commun.* **478**, 187–192.

Li, X., Egervari, G., Wang, Y., Berger, S.L., and Lu, Z. 2018. Regulation of chromatin and gene expression by metabolic enzymes and metabolites. *Nat. Rev. Mol. Cell Biol.* **19**, 563–578.

Lind, M.I., Missirlis, F., Melefors, Ö., Uhrigshardt, H., Kirby, K., Phillips, J.P., Söderhäll, K., and Rouault, T.A. 2006. Of two cytosolic aconitases expressed in *Drosophila*, only one functions as an iron-regulatory protein. *J. Biol. Chem.* **281**, 18707–18714.

Mercier, A., Watt, S., Bähler, J., and Labbé, S. 2008. Key function for the CCAAT-binding factor Php4 to regulate gene expression in response to iron deficiency in fission yeast. *Eukaryot. Cell* **7**, 493–508.

Mourer, T., Jacques, J.F., Brault, A., Bisaillon, M., and Labbé, S. 2015. Shu1 is a cell-surface protein involved in iron acquisition from heme in *Schizosaccharomyces pombe*. *J. Biol. Chem.* **290**, 10176–10190.

Mukherjee, K., Gardin, J., Futcher, B., and Leatherwood, J. 2016. Relative contributions of the structural and catalytic roles of Rrp6 in exosomal degradation of individual mRNAs. *RNA* **22**, 1311–1319.

Pelletier, B., Beaudoin, J., Mukai, Y., and Labbé, S. 2002. Fep1, an iron sensor regulating iron transporter gene expression in *Schizosaccharomyces pombe*. *J. Biol. Chem.* **277**, 22950–22958.

Pelletier, B., Beaudoin, J., Philpott, C.C., and Labbé, S. 2003. Fep1 represses expression of the fission yeast *Schizosaccharomyces pombe* siderophore-iron transport system. *Nucleic Acids Res.* **31**, 4332–4344.

Pelletier, B., Trott, A., Morano, K.A., and Labbé, S. 2005. Functional characterization of the iron-regulatory transcription factor Fep1 from *Schizosaccharomyces pombe*. *J. Biol. Chem.* **280**, 25146–25161.

Piccinelli, P. and Samuelsson, T. 2007. Evolution of the iron-responsive element. *RNA* **13**, 952–966.

Pouliot, B., Jbel, M., Mercier, A., and Labbé, S. 2010. *abc3+* encodes an iron-regulated vacuolar ABC-type transporter in *Schizosaccharomyces pombe*. *Eukaryot. Cell* **9**, 59–73.

Satoh, R., Morita, T., Takada, H., Kita, A., Ishiwata, S., Doi, A., Hagihara, K., Taga, A., Matsumura, Y., Tohda, H., *et al.* 2009. Role of the RNA-binding protein Nrd1 and Pmk1 mitogen-activated protein kinase in the regulation of myosin mRNA stability in fission yeast. *Mol. Biol. Cell* **20**, 2473–2485.

Shichino, Y., Otsubo, Y., Yamamoto, M., and Yamashita, A. 2020. Meiotic gene silencing complex MTREC/NURS recruits the nuclear exosome to YTH-RNA-binding protein Mmi1. *PLoS Genet* **16**, e1008598.

Telekawa, C., Boisvert, F.M., and Bachand, F. 2018. Proteomic profiling and functional characterization of post-translational mod-

ifications of the fission yeast RNA exosome. *Nucleic Acids Res.* **46**, 11169–11183.

Touat-Todeschini, L., Shichino, Y., Dangin, M., Thierry-Mieg, N., Gilquin, B., Hiriart, E., Sachidanandam, R., Lambert, E., Brettschneider, J., Reuter, M., *et al.* 2017. Selective termination of lncRNA transcription promotes heterochromatin silencing and cell differentiation. *EMBO J.* **36**, 2626–2641.

Volz, K. 2008. The functional duality of iron regulatory protein 1. *Curr. Opin. Struct. Biol.* **18**, 106–111.

Yamamoto, M. 2010. The selective elimination of messenger RNA underlies the mitosis-meiosis switch in fission yeast. *Proc. Jpn. Acad. Ser. B Phys. Biol. Sci.* **86**, 788–797.

Yamanaka, S., Yamashita, A., Harigaya, Y., Iwata, R., and Yamamoto, M. 2010. Importance of polyadenylation in the selective elimination of meiotic mRNAs in growing *S. pombe* cells. *EMBO J.* **29**, 2173–2181.

Yamashita, A., Shichino, Y., Tanaka, H., Hiriart, E., Touat-Todeschini, L., Vavasseur, A., Ding, D.Q., Hiraoka, Y., Verdel, A., and Yamamoto, M. 2012. Hexanucleotide motifs mediate recruitment of the RNA elimination machinery to silent meiotic genes. *Open Biol.* **2**, 120014.

Znaidi, S., Pelletier, B., Mukai, Y., and Labbé, S. 2004. The *Schizosaccharomyces pombe* corepressor Tup11 interacts with the iron-responsive transcription factor Fep1. *J. Biol. Chem.* **279**, 9462–9474.